

# Manipulating activated metabolism via mtorc1

2013

Ivan von Hack Prestinary  
*University of Central Florida*

Find similar works at: <https://stars.library.ucf.edu/honorstheses1990-2015>

University of Central Florida Libraries <http://library.ucf.edu>

 Part of the [Microbiology Commons](#), and the [Molecular Biology Commons](#)

## Recommended Citation

von Hack Prestinary, Ivan, "Manipulating activated metabolism via mtorc1" (2013). *HIM 1990-2015*. 1480.  
<https://stars.library.ucf.edu/honorstheses1990-2015/1480>

This Open Access is brought to you for free and open access by STARS. It has been accepted for inclusion in HIM 1990-2015 by an authorized administrator of STARS. For more information, please contact [lee.dotson@ucf.edu](mailto:lee.dotson@ucf.edu).

# MANIPULATING AKTIVATED METABOLISM VIA MTORC1

by

IVAN VON HACK-PRESTINARY

A thesis submitted in partial fulfillment of the requirements  
for the Honors in the Major Program in Biomedical Sciences  
in the Burnett School of Biomedical Science  
and in The Burnett Honors College  
at the University of Central Florida  
Orlando, Florida

Spring Term 2013  
Thesis Chair: Dr. Deborah Altomare

©2013 Ivan von Hack-Prestinary

## ABSTRACT

Although poorly understood, normal cells and cancerous cells of the same type exhibit different patterns of nutrient consumption, processing and utility of metabolic substrates. Differences in substrate uptake, preference, and alternately emphasized metabolic pathways offer opportunities for selective targeting of cancer versus stroma. This may be accomplished by using a sequential approach of nutrient deprivation and pharmaceutical perturbation of metabolic pathways to inhibit cellular proliferation. The purpose of this study was to investigate the effects of restricting glucose and glutamine concentrations, *in vitro*, to levels that resemble a potential human fasting state. The mammalian target of rapamycin (mTOR), a mediator of nutrient sensation, was then inhibited with rapamycin in the nutrient-restricted conditions. Because active Akt/mTOR is implicated in cancer cell pro-survival, the hypothesis is that pharmaceutical inhibition of active Akt/mTOR signaling in combination with the stress of restricted nutrient supply will be more effective than nutrient deprivation alone at disrupting metabolic processes to impair cancer cell proliferation and/or pro-survival mechanisms. Untreated and treated conditions were tested to determine if an additive or synergistic effect would result from a sequential insult of nutrient deprivation followed by inhibited mTORC1 signaling.

The cell line used for this study was cultivated from a murine pancreatic intraepithelial neoplasia (PANIN) derived from a transgenic mouse with pancreatic tissue-specific expression of constitutively active Akt. The transgene of Akt, isoform 1, contains a myristoyl tag that facilitates co-localization of Akt to the plasma membrane, thereby promoting the activation of this signaling protein. This aberrantly activated Akt represents a prosurvival condition observed

in most cancers, and impacts metabolic balance with increased downstream signaling to metabolic sensors and regulators, including mTORC1.

Several methods were used to evaluate changes in metabolic and physiological response to nutrient deprivation and mTORC1 inhibition. These included tetrazolium reduction/absorbance readings to qualitatively evaluate differences in cell proliferation, and Western immunoblots for observing changes in protein expression and phosphorylation. ATP luminescence assays were applied to quantify intracellular ATP content, and citrate synthase spectrophotometry used to quantify specific activity/indicate changes in the TCA/OXPHOS production of ATP. Results from the above methods suggest that, individually, nutrient deprivation and rapamycin treatment share some similar effects on metabolically-related protein phosphorylation and in reducing cellular proliferation. Collectively, nutrient deprivation plus rapamycin treatment, however, resulted in unanticipated metabolic alterations under conditions used for this study, the complexities of which would need to be delineated in future studies.

This work is dedicated to those who encouraged me to further my education, despite my protestations: Diane von Hack, Kyle Hoofnagle, Eugene Kowalski and Jeffrey Goldseth.

## **ACKNOWLEDGMENTS**

I would like to express profound gratitude to the members of my thesis committee, who have supplied me with superb instruction and constructive criticism. I especially would like to acknowledge my thesis chair, Dr. Deborah Altomare, whose patient mentorship has guided this project and my individual growth as a scientist. Special thanks also to Dr. Rebecca Boohaker, who provided indispensable input and supplied instruction in specialized lab technique applications. Finally, sincere thanks to Veethika Pandey who also helped in teaching laboratory technique, as well as offering a pair of helping hands when necessary.

## TABLE OF CONTENTS

ABSTRACT .....	iii
ACKNOWLEDGMENTS .....	vi
TABLE OF CONTENTS.....	vii
LIST OF FIGURES .....	ix
LIST OF ABBREVIATIONS/ACRONYMS.....	x
CHAPTER ONE: INTRODUCTION.....	1
Glycolysis .....	1
Tricarboxylic Acid Cycle/Oxidative Phosphorylation .....	2
Warburg Effect .....	3
Deregulated Glycolysis.....	6
Hexokinase.....	6
Pyruvate Kinase .....	7
Akt .....	9
mTOR .....	12
The Mitochondrion .....	14
Nutrient Restriction.....	16
Rationale and Hypothesis .....	17
CHAPTER TWO: MATERIALS AND METHODS .....	22



Cell Culture.....	22
Nutrient Restricted Media.....	22
Cell Partitioning/Distribution .....	23
Experimental Conditions .....	23
Cell Proliferation Assay.....	24
ATP Quantification.....	24
Isolation of Mitochondria .....	25
Citrate Synthase Assay .....	26
Western Blots.....	26
CHAPTER THREE: RESULTS .....	27
Reduction of formazan product in proliferation assays in rapamycin-treated conditions .....	27
Increased ATP concentrations in rapamycin-treated conditions .....	29
Increased specific activity of citrate synthase in rapamycin-treated conditions.....	30
Western immunoblots.....	33
CHAPTER FOUR: DISCUSSION.....	38
CHAPTER FIVE: CONCLUSION.....	44
Future Directions .....	44
LIST OF REFERENCES .....	46

## LIST OF FIGURES

Figure 1: Absorbance Readings of MTS/Formazan Post Rapamycin Treatment at 490nm.....	28
Figure 2: Molar ATP per Sample, Untreated vs. Treated .....	30
Figure 3: Mitochondrial Activity Assay, Citrate Synthase Specific Activity in International Units/ $10^6$ cells .....	32
Figure 4: Mitochondrial Integrity Assay, Citrate Synthase Specific Activity in International Units/ $10^6$ cells .....	33
Figure 5: phospho-70S6 kinase Western immunoblot, $\beta$ -actin control. ....	34
Figure 6: Semi-quantitative densitometry of phospho-S6 kinase. ....	34
Figure 7: phospho-Akt (Ser 473), $\beta$ -actin control.....	36
Figure 8: Semi-quantitative densitometry of phospho-Akt (Ser473). ....	36
Figure 9: phospho-Raptor (Ser 792), $\beta$ -actin control.....	37
Figure 10: Semi-quantitative densitometry of phospho-Raptor (Ser792).....	37

## **LIST OF ABBREVIATIONS/ACRONYMS**

4E-BP1: Eukaryotic translation initiation factor 4E-binding protein 1

ADP: Adenosine diphosphate

AMP: Adenosine monophosphate

AMPK: Adenosine monophosphate-activated protein kinase

ATP: Adenosine triphosphate

eIF4E: Eukaryotic translation initiation factor 4E

G-6-P: Glucose-6-phosphate

GSK3 $\beta$ : Glycogen synthase kinase -3 $\beta$

HK: Hexokinase

IGF: Insulin-like growth factor

IGF-1R: Insulin-like Growth Factor 1 Receptor

IRS-1: Insulin receptor substrate 1

mAkt1: Myristoylated Akt isoform 1

mTOR: Mammalian target of rapamycin

mTORC1, 2: Mammalian target of rapamycin complex 1, 2

NADH/NAD<sup>+</sup>: Nicotinamide adenine dinucleotide

OXPHOS: Oxidative Phosphorylation

PI3K: Phosphatidylinositide 3-kinases

PKM1,2: Pyruvate kinase M isoform 1,2

S6K: Ribosomal protein S6 kinase

TCA: Tricarboxylic acid cycle

5'TOP: 5'Terminal oligopyrimidine tract

TSC2: Tuberous sclerosis complex 2

VDAC: Voltage dependent anion channel

## CHAPTER ONE: INTRODUCTION

Metabolism encompasses the totality of chemical transformations that comprise the energetic and material basis for cellular life. This totality can be subdivided into two categories of activity: *catabolism*, or energy production, and *anabolism*, component production. *Cellular respiration* refers to the set of catabolic or energy-producing chemical transformations whereby metazoan cells convert organic compounds into the energy currency of the cell, adenosine triphosphate (ATP) and byproducts. Cellular respiration proceeds through a series of enzymatic pathways in order to process substrates into biochemical energy; the first of these pathways is termed *glycolysis*<sup>1</sup>.

### Glycolysis

Glycolysis is an oxygen-independent metabolic pathway that consumes carbohydrates, particularly glucose, as the substrate for energy production. This process occurs in the cytoplasm, and is comprised of a series of ten enzymatic reactions that convert one molecule of carbohydrate into two pyruvate molecules, reduce two nicotine adenine dinucleotide (NADH) coenzymes and generate two molecules of ATP. The resulting pyruvate molecules then have two potential fates, depending on whether molecular oxygen (O<sub>2</sub>) is present. In conditions where a sufficient concentration of O<sub>2</sub> is present in the intracellular space, the pyruvate can be transported into the mitochondria and oxidized into acetyl-CoA and CO<sub>2</sub>, a *transition step* that links the metabolic pathways of glycolysis and the tricarboxylic acid cycle (TCA). Alternately,

in *hypoxic*, or low O<sub>2</sub> concentration, or *anoxic* conditions where no O<sub>2</sub> is present, the pyruvate can be converted into lactic acid via a process termed *lactic acid fermentation*<sup>1</sup>.

### Tricarboxylic Acid Cycle/Oxidative Phosphorylation

The TCA is comprised of a cyclic series of eight enzymatic reactions, a process that occurs in the matrix of the mitochondria. These reactions convert one molecule of acetyl-CoA into two molecules of CO<sub>2</sub> and H<sub>2</sub>O, and subsequently reduce three molecules of NAD<sup>+</sup> to NADH and one molecule of ubiquinone (Q) to ubiquinol (QH<sub>2</sub>). These reduced coenzymes then transfer their electrons into the *oxidative phosphorylation* (OXPHOS) pathway. As the coenzymes release electrons into the *electron transport chain* (ETC) of the OXPHOS pathway, a proton gradient is established across the cristae membrane in the mitochondria. The potential produced by the proton gradient yields a *proton motive force* that drives the formation of ATP from adenosine diphosphate (ADP) and inorganic phosphate via the ATP synthasome<sup>2,3</sup>. Oxygen couples TCA and OXPHOS by accepting the electrons generated by TCA which are transported through the electron transport chain of OXPHOS; O<sub>2</sub> is reduced and converted to H<sub>2</sub>O at the terminus of the ETC. Thus, oxygen ultimately receives the electrons transferred from the carbohydrate substrate, and fundamentally links the metabolic pathways of glycolysis, TCA and OXPHOS in a process referred to as *aerobic respiration*<sup>3</sup>.

In hypoxic or anoxic conditions, insufficient O<sub>2</sub> inhibits the efficient consumption of pyruvate via aerobic respiration; in such anaerobic conditions, *anaerobic respiration* results. In

conditions where pyruvate accumulates, the redox state of the cell changes due to the corresponding concentration increase of NADH and decrease of NAD<sup>+</sup>. To restore the redox state, the accumulated pyruvate requires conversion by lactic acid dehydrogenase and NADH into lactic acid via lactic acid fermentation<sup>1</sup>.

In normal cells, the constituent pathways of aerobic respiration, glycolysis, TCA and OXPHOS are tightly coupled. Carbohydrates are first consumed through the energetically low-yield glycolysis, and the end product of pyruvate then processed through TCA/OXPHOS for a high yield of ATP<sup>1,3</sup>. In conditions of hypoxic exertion or anoxic ischemia, anaerobic respiration uses lactic acid fermentation to continue a reduced production of biochemical energy. Cancer metabolism, however, differs markedly from normal cellular metabolism, and demonstrates different rates and activity of the catabolic and anabolic pathways versus normal cells of the same type<sup>4</sup>.

### Warburg Effect

Metabolic differences between normal and cancerous tissues were reported in 1924 by Otto Warburg et al. Warburg used a manometer to quantify oxygen consumption in thin slices of tissue. The manometer was additionally equipped to measure carbon dioxide (CO<sub>2</sub>) emission, which correlated to lactic acid (C<sub>3</sub>H<sub>6</sub>O<sub>3</sub>) production in a bicarbonate (HCO<sub>3</sub><sup>-</sup>) buffer according to the formula: C<sub>3</sub>H<sub>6</sub>O<sub>3</sub> + HCO<sub>3</sub><sup>-</sup> → C<sub>3</sub>H<sub>5</sub>O<sub>3</sub><sup>-</sup> + H<sub>2</sub>O + CO<sub>2</sub>. Results from the manometric measurements indicated that cancerous tissue generated lactic acid even in aerobic, or

oxygenated conditions<sup>5, 6</sup>. The generation of lactic acid in aerobic conditions, due to the conversion of pyruvate, indicated a deregulation of either glycolysis or OXPHOS.

The measured O<sub>2</sub> consumption, however, was determined to be the same in the normal and cancerous tissues. Despite these results, Warburg asserted:

“The origin of cancer lies in the anaerobic metabolic component of normal growing cells, which is more resistant to damage than is the respiratory component. Damage to the organism favours this anaerobic component and, therefore, engenders cancer.<sup>6,7</sup>”

Thus, Warburg hypothesized that the aerobic production of lactic acid was related to a damaged respiratory system (TCA/OXPHOS). Later studies have correlated instances of aerobic glycolysis with mitochondrial damage or depopulation; such instances, however, do not account for deregulation of the glycolytic pathway, a possibility Warburg discounted<sup>6,8,9</sup>.

Evidence for a cancerous metabolic shift in favor of glycolysis was supplied by a genomic study of a set of 24 cancers, representing greater than 70% of human cancer cases globally. The authors state, “in glycolysis the overexpression of genes is the rule rather than the exception,” finding 62% of possible overexpressions of genes in the glycolysis pathway were indeed overexpressed<sup>10</sup>. Reliance of cancerous cells on the low ATP-yielding glycolysis pathway in contradistinction to the higher ATP-yield of aerobic respiration appears paradoxical; however, the rate of ATP production from glycolysis is approximately 100 times faster than from



oxidative phosphorylation<sup>11</sup>. Warburg described the difference between the metabolic emphases of cancerous versus normal cells:

“This converted to energy equivalents means that the cancer cells can obtain approximately the same amount of energy from fermentation as from respiration whereas the normal body cells obtain much more energy from respiration than from fermentation<sup>12</sup>”

The comparatively rapid rate of glycolysis versus TCA/OXPHOS supplies cancer cells with a competitive advantage versus normal cells for a shared energy resource, glucose<sup>11</sup>. Despite relative energy production equivalence, in the cancerous metabolic condition where lactic acid fermentation is *not* suppressed by the presence of O<sub>2</sub>, additional metabolic byproducts are produced by the glycolytic pathway. These byproducts are processed by the pentose phosphate pathway, supplying precursors for the biosynthesis of nucleic acids, phospholipids, fatty acids, cholesterol, and porphyrins<sup>13</sup>. Upregulated glycolysis, and consequently precursor byproducts, promotes an increased supply of cellular components and facilitates proliferation. Another additional benefit conferred by the cancerous reliance on glycolysis consists of the reduced cellular requirement for O<sub>2</sub>, an important protection in conditions of ischemia produced by rapidly proliferating cells<sup>13</sup>.

## Deregulated Glycolysis

Enzyme isoforms in the cancerous glycolytic pathway exert disproportionate influence on the transfer of intermediates into accessory processing pathways, as well as the overall reaction rate of glycolysis. Deregulated activity of the glycolytic pathway appears to be mostly attributable to isoforms of two enzymes, one at the beginning of the pathway, the other at the end. Hexokinase (HK), the first enzyme in the glycolytic pathway, phosphorylates glucose according to the formula:  $\text{Glucose} + \text{ATP} \rightarrow \text{Glucose-6-PO}_4^{2-} + \text{ADP}^{1,14}$ . This reaction accomplishes a dual function in maintaining a low intracellular concentration of glucose while preventing the export of the phosphorylated carbohydrate product from the intracellular space<sup>15</sup>.

## Hexokinase

Four isoforms of HK have been identified in mammalian tissue, denoted HK I, HK II, HK III, and HK IV (also termed *glucokinase*). Tissues such as liver and pancreas express HK IV under normal conditions; this particular isoform has a much higher  $K_m$  (~5mM) than the  $K_m$  of HK I, II and III (~0.02mM). Thus HK I, II and III demonstrate an affinity for substrate 250 times greater than HK IV, increasing the relative reaction rate whereby glucose is phosphorylated. HK isozymes are expressed depending on cellular conditions: HK I mediates the phosphorylation of glucose in non-dividing cells, alternately, HK II is induced and performs the same function in proliferating cells; in tumorigenesis of liver and pancreatic tissues, a

“switch-over” of HK IV to HK II occurs, with a corresponding silencing of HK IV (glucokinase) expression<sup>15,16,17,18</sup>.

The hexokinase isozymes localize differently in the cell, with glucokinase localized in the nucleus in complex with the *glucokinase regulatory protein* (GKRP). Increases in intracellular glucose concentrations in hepatocyte and pancreatic  $\beta$ -cells result in HK IV-GKRP disassembly and translocation of HK IV to the cytoplasm, where the enzyme attaches to insulin granules, with a small fraction of HK IV possibly associating with outer mitochondrial membranes<sup>19,20,21</sup>. No evidence for a regulatory protein of either HK I or II has been documented; these hexokinases also preferentially populate the outer mitochondrial membrane, binding to the *voltage dependent anion channel* (VDAC)<sup>22</sup>. Binding to the mitochondrial membrane by HK I & II facilitates substrate channeling of intra-mitochondrially generated ATP to the hexokinase<sup>23,24</sup>. HK I & II translocation and binding to the mitochondrial membrane also reduces the sensitivity of the isoenzymes to allosteric inhibition by their product glucose-6-phosphate (G6P)<sup>25,26</sup>. Thus, four factors, the absence of a specific regulatory protein, a lower  $K_m$  compared to glucokinase, localization to a source of substrate, and reduced product inhibition generate an advantageous combination for HK II to disrupt the dynamic balance between glycolysis and TCA/OXPHOS.

### Pyruvate Kinase

The enzyme responsible for catalyzing the final step of glycolysis is *pyruvate kinase* (PK). This transferase catalyzes the transfer of a phosphoryl from phosphoenolpyruvate to ADP,

generating one ATP and one molecule of pyruvic acid. Just as a variety of hexokinase isozymes are expressed depending on cellular conditions, pyruvate kinase has tissue-specific isoforms such as *PKL*, found in gluconeogenic tissues such as liver and kidneys, *PKR*, found in erythrocytes, as well as *pyruvate kinase M isoform 1* (PKM1), found in metabolically demanding tissues such as muscle and brain<sup>27</sup>. Pyruvate kinase isoform 2 (PKM2) has been observed to be expressed in normal differentiated tissues, including fat, lung and retinal, as well as pancreatic islets<sup>28</sup>. PKM2 has been characterized as the isoform expressed in cells with high rates of nucleic acid synthesis, i.e. proliferating cells. The expression of PKM2 is thus found almost universally in proliferating cells, though not necessarily the exclusive isoform present, in normal and embryonic tissues, with higher expression of this splice variant found in cancerous cells<sup>27</sup>.

Non-proliferating, differentiated cells rely on the efficient ATP generation of TCA/OXPHOS, a catabolic optimization of bioenergetic precursors in competitive metazoan conditions of limited growth factor supply<sup>29</sup>. Proliferating cells, alternatively, depend less on maximization of ATP yield and instead emphasize metabolic intermediate/precursor flux into anabolic pathways<sup>30</sup>. One means of this precursor diversion into macromolecular synthetic pathways is driven by the expression the glycolytic isoform HK II, which generates the metabolic intermediate glucose-6-phosphate (G-6-P) at a greater rate due to mitochondrial localization and faster reaction rate. PKM2 also facilitates anabolic metabolism via a switchable, reduced reaction rate versus PKM1, promoting the accumulation of upstream glycolytic intermediates, which are then shunted to anabolic pathways branching from the glycolytic pathway<sup>30</sup>.

Unlike PKM1, which exists solely as a highly enzymatically active tetramer, PKM2 has two forms: a tetramer with high affinity for phosphoenolpyruvate (PEP), and a dimer with low PEP affinity<sup>31</sup>. The PKM2 tetramer:dimer ratio determines the direction of substrate flux: when the tetramer predominates, PEP is converted to pyruvate, available for lactic acid fermentation or TCA/OXPHOS; in contrast, the enzymatically inactive dimer introduces a glycolytic bottleneck, requiring the shunting of glycolytic intermediates into branching synthetic pathways<sup>31</sup>. Byproducts of the branching synthetic pathways, such as reactive oxygen species (ROS) generated from the pentose phosphate pathway, inactivate the PKM2 tetramer<sup>32</sup>. Additional down-regulatory mechanisms for PKM2 have been found, including inhibition of tetramer formation due to tyrosine phosphorylation (Y105), and chaperone-mediated autophagy via acetylation of a specific lysine (K305) on PKM2 in high glucose environments<sup>33,34</sup>. As a result, PKM2 function oscillates depending on tetramer:dimer ratio, controlled by ROS and phosphotyrosine inactivation, as well as context-dependent degradation. PKM2 thus provides the proliferating cell a responsive, regulatory switch between energy maximization and anabolic synthesis in the glycolytic phenotype<sup>29,30,31</sup>.

### Akt

The Akt kinase family functions as a downstream effector of growth factor signaling pathways, and is activated by membrane bound phosphoinositol-3-kinase (PI3K)-dependent mechanisms. Akt is a serine/threonine kinase, expressed as three isoforms, and has been documented as frequently hyperactivated across a broad variety of tumor types<sup>35,36</sup>. Akt exerts

pleiotropic effects that can facilitate tumorigenesis and cancer cell survival, modulating proliferation, prosurvival mechanisms and intermediate metabolism<sup>35,37</sup>. Of the three isoforms, Akt1 and Akt2 appear particularly relevant to the processes of cancer metabolism and survival.

Hyperactivity of Akt in cancer has been associated with increased glycolysis, in part due to increased expression levels of GLUT1 and inducing increased translocation of GLUT4 to the plasma membrane<sup>39,43</sup>. Additionally, Akt activation has been demonstrated to increase the binding of hexokinase to the mitochondria<sup>40</sup>. Akt can directly phosphorylate hexokinase II; this phosphorylation has been demonstrated in cardiomyocytes to increase the binding of HK II to the voltage dependent anion channel (VDAC) in the outer mitochondrial membrane<sup>39</sup>.

Another metabolic regulation effected by Akt results from Akt phosphorylating glycogen synthase kinase 3 beta (GSK3 $\beta$ ) on serine 9, inactivating GSK3 $\beta$ <sup>38</sup>. This inactivation is significant in the coupling of glycolysis and TCA/OXPHOS as GSK3 $\beta$  phosphorylates the VDAC, which occludes the binding site for HK II, preventing hexokinase binding to the mitochondrial membrane. Upregulated AKT activity increases the inhibitory phosphorylation of GSK3 $\beta$ , facilitating the binding of HK II to the mitochondrial membrane<sup>38</sup>. The Akt-mediated binding of HK II to the mitochondrial membrane directs HK II activity in favor of glycolysis, due largely to the channeling of the intra-mitochondrial ATP to HK II as well as the reduced sensitivity of HK II to the inhibitory product G-6-P when attached to the mitochondrial membrane<sup>23,24</sup>. An additional prosurvival effect is obtained by having HK II bind the VDAC,

preventing the closure of the VDAC and thereby inhibiting the formation of the mitochondrial transition pore in response to stress and hypoxic conditions<sup>38</sup>.

Using polymerase chain reaction, genes that encode for an Akt have been modified with a src myristoylation sequence, which have been transfected into specialized mouse lines via recombinant DNA technology<sup>42</sup>. Myristoylated Akt (mAkt) demonstrates constitutive activity *in cellulo*, as the myristoyl facilitates Akt adhesion to the plasma membrane, promoting the dual phosphorylation required for full activation of the kinase<sup>43</sup>. Constitutive Akt activity decouples the cell from dependence on growth factor-initiated signal transduction, inducing an autonomous proliferative signaling cascade<sup>30</sup>. Additional metabolic changes attributable to mAkt/hyperactivated Akt beyond increased glucose flux include constitutive lipogenesis (a building block for necessary for proliferation) and enhancement of insulin-stimulated glycogen synthesis, due to Akt-mediated inhibition of GSK3 $\beta$ <sup>43</sup>.

Akt also promotes cell growth by facilitating the activation of the mammalian target of rapamycin (mTOR). This facilitated activation results from Akt-mediated phosphorylation of negative regulators of mTOR, including tuberous sclerosis complex 2 (TSC2) and the proline-rich Akt substrate of 40kDa (PRAS40)<sup>44,45</sup>. Phosphorylation of TSC2 promotes complexation with TSC1, which together act as a GTPase-activating protein for the Rheb protein, which activates mTOR complex 1 (mTORC1) when Rheb has GTP bound<sup>44,46</sup>. PRAS40 associates with mTORC1 and has been found to negatively regulate mTORC1 signaling; phosphorylation

of PRAS40 by Akt inhibits the negative regulation imposed by PRAS40 when in complex with mTORC1<sup>44,47</sup>.

### mTOR

The mammalian target of rapamycin (mTOR) is a serine/threonine kinase that integrates inputs from energy status signals, oxygen and amino acid concentrations, as well as growth factor signaling downstream from Akt, functioning as a switch for anabolic and catabolic processes<sup>48</sup>. mTOR nucleates two distinct multiprotein complexes, referred to mTOR complexes 1 and 2 (mTORC1, mTORC2).

mTOR acts as the master negative regulator in an essential process of cell regulation and survival, autophagy<sup>52</sup>. mTOR complex 1 integrates nutrient availability and growth factor signals, mediating the balance between cell growth and autophagy. Given nutrient-sufficient conditions, mTORC1 inactivates the nucleation of phagophores, thereby repressing the autophagic process. In restricted nutrient conditions, however, mTORC1 activity becomes inhibited, which de-suppresses autophagy, allowing the cell to mobilize intracellular resources through decomposition of proteins and organelles to cellular building blocks<sup>53</sup>.

Conditions of glucose starvation reduce the intracellular ratio of metabolically generated ATP versus adenosine monophosphate (AMP); increases of AMP concentration relative to ATP can result in the activation of the energy status sensor *5' adenosine monophosphate-activated*



*protein kinase* (AMPK), depending on the cell type. In particular, glucose sensing cells that express the glucose transporter GLUT2 and glucokinase, such as pancreatic beta cells, AMPK is regulated by fluctuations in available glucose<sup>55</sup>. Activated AMPK inhibits mTORC1 by phosphorylation/activation of TSC2, which, in activated state, negatively regulates mTORC1. AMPK also inhibits mTORC1 via direct phosphorylation mTORC1-associated protein Raptor. Just as mTOR negatively regulates autophagy, the negative regulation of mTORC1 by AMPK corresponds to a positive regulation of autophagy<sup>53,54,55</sup>.

mTOR also plays a key role in translation of mRNA, functioning as an anabolic regulator sensitive to amino acid concentrations<sup>60</sup>. This role is fulfilled by transducing growth factor signaling from Akt to ribosomal protein kinase S6 kinase (S6K) and the eukaryotic translation initiation factor 4E (eIF4E)-binding proteins (4E-BP1, 2, 3)<sup>56,58</sup>. 4E-BP1 is phosphorylated/inactivated by mTORC1, which induces the disassociation of the binding protein from the eIF4E. The released translation initiation factor is then free to bind eIF4G, which commences protein translation<sup>57,58</sup>.

Inhibition of mTORC1 via rapamycin prevents downstream phosphorylation/activation of S6K, and consequently ribosomal protein S6 (rpS6). Inhibition of rpS6 induces a partial inhibition of translation initiation of 5' terminal oligopyrimidine tract (5'TOP) mRNAs, attributable to a reduction in the inactivated rpS6's affinity for 5'TOP mRNAs<sup>59</sup>. Consequently, partial inhibition of the 5'TOP mRNAs via rapamycin inhibition of mTORC1 signaling results in a reduction of protein translation. Phosphorylation/dissociation of 4E-BP1 from eIF4E also

demonstrates a decremental response to rapamycin-mediated inhibition of mTORC1, contributing to a reduction in dissociated eIF4E and consequently protein translation<sup>61</sup>. Notably, the effect of rapamycin on inhibition of mTORC1 appears to depend on concentration, with S6K suppressed at nanomolar doses, and eIF4E at micro-molar doses<sup>61,62</sup>.

The Akt/mTOR pathway is activated by growth factors such as insulin and insulin-like growth factor 1 (IGF1), which bind both insulin and IGF1 receptors. These activated receptors then phosphorylate insulin receptor substrates 1 and 2 (IRS1, 2), which transduce signal to Akt via PI3K. Activated Akt via IRS1,2 then indirectly activates mTOR through TSC2 and PRAS40 phosphorylation. Activation of mTOR consequently mediates a feedback down-regulation of the PI3K/Akt/mTOR pathway by inducing a loss of IRS1 expression through S6K<sup>49</sup>. In conditions of nutrient satiety, S6K is activated, which has been shown to negatively regulate insulin signaling; this down-regulation facilitates the suppression of insulin signaling through IRS phosphorylation by S6K, ultimately traceable to mTORC1 activity<sup>51</sup>. Alternately, in conditions of mTOR inhibition via rapamycin, IRS1 protein levels have been found in a number of tumor cell lines to be upregulated, which induces Akt phosphorylation and consequent upregulation of Akt kinase activity<sup>49</sup>.

### The Mitochondrion

The mitochondrion is an organelle composed of a permeable outer membrane, perforated by porins, and an impermeable inner membrane. The inner membrane of the mitochondrion

contains the mitochondrial matrix, wherein the enzymes of the TCA cycle oxidize acetyl-CoA to CO<sub>2</sub>, generating GTP, NADH and FADH<sub>2</sub>. The reduced coenzymes NADH and FADH<sub>2</sub> provide the electrons and protons for perpetuating the OXPHOS electronic and protonic gradients. The electrons are transported through four complexes in the electron transport chain, ensconced in the inner mitochondrial membrane, and ultimately reduce molecular oxygen into water. The protons from the coenzymes are transported across the inner mitochondrial membrane; the gradient then refluxes through the ATP synthasome to generate ATP from ADP and inorganic phosphate<sup>3,63,64</sup>.

mTOR has been implicated in coordinating mitochondrial activity with growth regulation. A study examining the effect of mitochondrial dysfunction on mTOR found that mTOR was largely co-localized with the outer membrane of the mitochondria<sup>65</sup>. Another study using Jurkat cells determined that the inhibition of mTORC1 using rapamycin resulted in decreases in mitochondrial membrane potential, reduced oxygen consumption and overall oxidative capacity, fundamentally altering the metabolic rate of the treated cells<sup>66</sup>. Schieke et al. discovered that mTORC1 inhibition did not induce significant changes in the expression levels of OXPHOS-associated proteins. The OXPHOS-associated proteins, however, exhibited isoelectric shifts indicative of dephosphorylation in the rapamycin-inhibited conditions. Conservation of protein expression in tandem with dephosphorylation in mTORC1-inhibited conditions indicates an mTOR-mediated regulation of the OXPHOS phosphoproteome<sup>66</sup>. Mitochondrial function can also influence mTOR activity via a process termed retrograde signaling; this reciprocal regulation by mitochondria can issue a down-regulatory signal to mTOR in the event of lowered membrane potential<sup>65,66,67,68</sup>.

Ramanathan and Schreiber discovered an immediate change in mitochondrial function after inhibition of mTOR. Rapamycin-treated leukemic cells were observed to demonstrate reduced mitochondrial function, with a corresponding upregulation of aerobic glycolysis; these changes were tracked within a 25 minute experimental window<sup>69</sup>. Notably, the authors observed an increase of amino acid concentrations, including arginine, histidine, proline, isoleucine, methionine, valine, phenylalanine and tyrosine, all of which may be converted to TCA cycle intermediates via the process of anaplerosis. Additionally, immunoprecipitations performed as part of the study revealed that mTOR co-immunoprecipitates with the mitochondrial VDAC and Bcl-xl. mTOR therefore appears to be integrally connected with mitochondrial function, particularly with respect to the VDAC, also a binding site for HK II<sup>22,69</sup>.

### Nutrient Restriction

Hirayama et al. conducted a metabolomics analysis of human colon and gastric cancers, finding very low glucose and correspondingly high lactate and glycolytic intermediate concentrations<sup>70</sup>. Intratumoral tissue amino acid concentrations were also found to be elevated, with glutamate present in the highest concentrations. Glutamine, however, was determined to be at levels near normal tissues. The excess of glutamate indicated a high flux of glutamine consumption, as cancer cells frequently act as “nitrogen traps”, competing against the host for glutamine to oxidize and for protein synthesis<sup>69</sup>. Glutamine is secondary only to glucose in cancer cell metabolism; it has the highest concentration of any amino acid in human plasma, and cancer cells metabolize more glutamine than any other amino acid<sup>72,73,74</sup>.

Poor vascularity and upregulated amino acid biosynthesis insufficiently accounted for the excess essential amino acid concentrations in the tumors studied; evidence for autophagy was indicated by excesses of hydroxyproline, a byproduct of autophagic degradation of collagen<sup>70</sup>. Indeed, activated autophagy has been associated with pancreatic cancer cells as a response to poor vascularization, with the attendant effects of hypoxia and nutrient insufficiency<sup>72</sup>.

### Rationale and Hypothesis

The flux of nutrients available to cancerous cells affects the metabolic mechanisms emphasized for growth, proliferation and survival<sup>70,71,75,76</sup>. Nutritional context also impacts the effect of anticancer agents on cancerous cells; an *in vitro* study by Lu et al. found vincristine, 5-fluorouracil, taxol, doxorubicin, cisplatin, and camptothecin killed human cancer cell lines in nutrient sufficient media, but exerted significantly reduced cytotoxicity in nutrient-restricted media<sup>77</sup>. Since nutrition can impact cancer metabolic mechanisms and anticancer drug effectiveness, it may offer a leveragable variable to target and damage cancerous cells versus normal cells.

The PI3K-Akt-mTOR pathway provides the cell with essential signaling with respect to growth, proliferation and cell survival. However, this pathway may be converted to a pro-death signal, driving cells to necrosis or nonapoptotic cell death in response to metabolic stress. Activation of PI3K/Akt via insulin and IGF-1 in glucose restricted contexts has been demonstrated to result in inhibition of autophagy and consequent autophagic cell death in rat

cardiomyocytes<sup>78</sup>. Wu et al. have supplied further evidence for the mechanism of activated PI3K-Akt-mTOR signaling suppressing the prosurvival effects of autophagy and promoting necrotic cell death in cells subjected to starvation conditions<sup>79</sup>.

The cells used for this experimental inquiry were harvested from a murine pancreatic lesion; this cell line is remarkable in that the specimen was culled from a transgenic mouse, expressing an ectopic myristoylated Akt1 (mAkt1) in its pancreatic tissues. The presence of this ectopic mAkt1 induces a condition of constitutive Akt1 activation, due to the membrane recruitment facilitated by the myristoyl modification. This state of constitutive activation provides a simulated context for the majority of cancer cells that exhibit hyperactivated Akt<sup>35,36</sup>.

Cells that express activated Akt exhibit enhanced proliferation and upregulated nutrient intake. Cancerous cells, likewise, develop competitive metabolic phenotypes, relative to normal cells, that support proliferative modalities. Cancerous cells quickly generate a nutrient-deprived context, relative to normal tissues, due to the de-regulated proliferation generated by the competitive metabolic phenotypes. Indurated tumor mass formation creates a context characterized by deprivation of vascular delivery of O<sub>2</sub>, glucose, amino acids and growth factors. Thus the cells comprising the tumor mass adapt to a situation of nutritional insufficiency, adopting phenotypes that optimize energy and cellular building block production from metabolic intermediates.

The original research proposal consisted of two conceptual parts. The first part of the original concept involved a comparative set of experiments to evaluate cell line response to restricting the essential nutrients glutamine and glucose. Growth media was compared to two minimal media preparations, one with glucose concentrations equal to growth media, and one that approximated human physiological fasting glucose concentrations. Both minimal media preparations had reduced glutamine concentrations, relative to growth media, and approximated human physiological fasting levels of glutamine. The rationale behind the reduction of nutrient supply was to determine if inducing a fasting state would impose a cytostatic, autophagic or apoptotic response in the cell lines. By extension, nutrient restriction *in vivo* would further reduce the already restricted nutrients supplied to cancerous cells in tumor formation.

The second main part of the original proposal concept involved mTOR inhibition via rapamycin. The thrust of this inquiry was inspired by a study performed by Lashinger et al., comparing differences in pancreatic tumor formation in mice treated with dietary versus pharmacologic interventions. Results from the study found that both chronic calorie restriction and rapamycin-mediated inhibition of mTOR decreased pancreatic tumor growth; however, calorie restriction was associated with reductions in pro-survival signaling, while rapamycin treatment did not mimic this effect. Calorie restriction (CR) in the mice was found to result in pleiotropic effects, inducing systemic reductions in circulating hormones IGF-1 and leptin production, while also reducing tumor cell expression of phospho-Akt, mTOR and IGF-1R<sup>80</sup>. Contrarily, selective inhibition of mTOR with rapamycin did not significantly impact hormonal production versus controls.

In cells with an activated Akt condition, mTOR inhibition removes regulatory repression of autophagy, with indications that the cell compensates for mTOR inhibition by up-regulating IGF-1R and IRS-1. Upregulation of this receptor and key signaling enzyme increase the cellular capacity for the uptake of growth factors, which activate the PI3K-Akt-mTOR pathway. As activated Akt has the potential to act as a pro-death signal, a *combined* treatment including mTOR inhibition and nutrient restriction may lever the pathway away from prosurvival activity, leading instead towards necrosis.

Restricting nutrients imposes a condition of metabolic stress on the cell; pancreatic cancer cells have previously been demonstrated to include autophagy as an integral contribution to the proliferative metabolic repertoire<sup>72</sup>. When the cell is already in a condition where it relies on autophagy for survival in conditions of reduced nutrient supply, excess reliance imposed by severe nutritional restriction may further contribute to the induction of a necrotic process. Rapamycin treatment removes the regulatory suppression of autophagy, which may accelerate autophagic processes in conditions of metabolic stress. Integrating the concepts of nutrient restriction, to induce metabolic stress, in combination with rapamycin treatment, to de-suppress or increase the activity of autophagy, generated the *hypothesis* of this study: a combination treatment of nutrient restriction and rapamycin inhibition will exert an additive or synergistic cytostatic/cytotoxic effect *in vitro* on the mAkt1 pancreatic neoplasia cell line. In support of this hypothesis, Sun et al. achieved synergistic reductions in the proliferation and tumor development of cells with hyperactive mTOR by employing a strategy of dual suppression of mTOR and glycolysis using rapamycin and 3-bromopyruvate<sup>80</sup>.



One of the mechanisms used for the support of this hypothesis was driven by Ramanathan and Schreiber's discovery that mTOR inhibition with rapamycin induced immediate changes in mitochondrial function, with energetic production shunted from mitochondrial to glycolytic mechanisms<sup>69</sup>. This metabolic shift may possibly be linked to mTOR functioning as a positive regulator for the glycolytic isoenzyme PKM2; paradoxically, however, hyperactive mTOR has been correlated with promotion of aerobic glycolysis<sup>81</sup>. As Ramanathan and Schreiber constrained their metabolic assays to the immediate and 25-minute post incubation with rapamycin responses, their results may indicate a transitional phase of metabolic readjustment. An experimental model that includes pre-conditioning to new nutritional concentrations, followed by assays taken after a more extended incubation with rapamycin was consequently developed for this project. Extending the interval of treatment provides data that indicates the stability of the immediate and short-term metabolic changes observed by Ramanathan et al.

## CHAPTER TWO: MATERIALS AND METHODS

### Cell Culture

A transgenic murine cell line cultured from a pancreatic lesion, and expressing mAkt1 (P177), was used for all following experiments. The cells were cultured in growth media consisting of Dulbecco's Modified Eagle's Medium (DMEM, Corning Cellgro) with 100 U/mL penicillin, 100 µg/mL streptomycin, 2mM glutamine and 10% fetal bovine serum (FBS, Atlanta Biologicals) added, in 5% CO<sub>2</sub> AT 37 °C.

### Nutrient Restricted Media

Minimal media first prepared using 900mL of deionized water added to a 1000mL beaker, with 1 vial of Dulbecco's Modified Eagles Base powder (Sigma, D5030). 3.7g of sodium bicarbonate were added, and pH adjusted using 1M NaOH or 1M HCl. Final volume brought to 1000mL total, then solution immediately filtered. 0.1M glucose solution was prepared using 100mL prepared minimal media with 1.802g dextrose and filtered. Concentration formula,  $V_1C_1=V_2C_2$   $V_1(0.1M C_6H_{12}O_6) = (V_2 mL)(C_2 C_6H_{12}O_6)$ , was applied to determine quantities of high-concentration glucose media required to prepare 4mM and 25mM glucose media preparations, respectively. 200mM glutamine solution was diluted into prepared glucose conditions using concentration formula to produce 0.7mM glutamine.

### Cell Partitioning/Distribution

Cells were trypsinized and collected in a 50mL conical tube and quenched in 3x volume of DMEM 10% FBS, then centrifuged at 1100 g for 5 minutes to form a pellet. After centrifugation, supernatant was aspirated, and cells resuspended in 2mL DMEM by trituration. Cell concentration was determined using a BioRad TC10 cell counter and dual chamber counting slides (BioRad). Cell count provided by the TC10 enabled concentration determination by number of cells/mL; using  $C_1V_1=C_2V_2$ , the volume necessary to transfer  $8.3 \times 10^3$  cells/cm<sup>2</sup> from the concentrated cell suspension to new 10cm diameter dishes (TPP). The concentrated cell solution was transferred to the 10cm dish pre-dispensed with sufficient media to bring final volume of DMEM to 10mL.

### Experimental Conditions

Each experiment involved two sets of conditions, untreated and treated with 20nM rapamycin. Each set was initially prepared the same, with  $8.3 \times 10^3$  cells/cm<sup>2</sup> distributed per 10cm dish into DMEM 10% FBS 25mM glucose 2mM glutamine media and allowed to seat for 24 hours. In each set, media was then aspirated and replaced, with one dish receiving DMEM growth media, the second dish 25mM glucose/0.7mM glutamine minimal media, and third dish 4mM glucose/0.7mM glutamine minimal media, respectively. The dishes were then allowed to accommodate to new media conditions for 24 hours. Following this step, 100mM rapamycin was added to the media in the rapamycin-treated set of dishes to yield a 20nM concentration; the cells in both conditions were then incubated for an additional 24 hours. After a total of 72 hours

preparation, the cells, whether in 96-well plate, 6-well plate or 10cm tissue culture dishes were prepared for experimental assay.

### Cell Proliferation Assay

Cells were harvested via trypsinization, counted in a BioRad TC10 cell counter, and distributed 5000 cells/well with a multichannel pipette into a 96 well plate. Cells were given a 12 hour period to seat in DMEM media, following which the DMEM was aspirated and replaced with fresh DMEM, 25mM and 4mM in untreated conditions and with fresh DMEM, 25mM, 4mM containing 20nM rapamycin for treated conditions. Cells were then allowed to incubate at 5% CO<sub>2</sub> 37 °C in these new conditions for 24 hours. Cell proliferation/cytotoxicity was evaluated using a colorimetric CellTiter 96® AQueous One Solution Cell Proliferation Assay (Promega). Each well contained 100µL culture media, to which 20µL MTS reagent was added and incubated at 5% CO<sub>2</sub> 37 °C for two hours. The resulting absorbance was then recorded at 490nm using an EnVision Multilabel Reader (PerkinElmer).

### ATP Quantification

Cells were prepared in 6-well dish as described in the Experimental Conditions section. Cells were trypsinized, quenched, centrifuged at 1100 rpm for 5 minutes, aspirated and resuspended in 1mL appropriate media and counted using a BioRad TC10 cell counter. A multichannel pipette was then used to distribute 5000 cells/well into a black 96-well plate, in triplicate per condition, with final volume of well brought to 100µL total with the condition-

appropriate media. An ATPlite ATP detection assay system set of reagents were used to determine ATP concentration by luminescence (PerkinElmer); luminescence was recorded by an EnVision multiplate reader (PerkinElmer).

### Isolation of Mitochondria

Cells were prepared as described in Experimental Conditions, with production scaled to yield a minimum of  $10 \times 10^6$  cells per condition. Cells were trypsinized, quenched in 3x volume of DMEM 10% FBS, then centrifuged at 1100 g for 5 minutes to form a pellet. Media was aspirated from the pellets, which were resuspended in 2mL fresh media of the same composition as incubation; if rapamycin treated, rapamycin was present at 20nM. The cells were then counted using TC10 cell counter to determine total cell count. The smallest count of total cells amongst the conditions established the total cell number cap for all conditions. The cell suspensions were then dispensed to 2mL microcentrifuge tubes, maintaining equal cell count totals across conditions according to the cell number cap, and brought to 2mL volume with PBS. The microcentrifuge tubes were then centrifuged at 700 g for 2 minutes. Media/PBS was then aspirated and cells triturated in PBS and re-centrifuged at 700g for another 2 minutes. Cells were then prepared with a Mitochondria Isolation Kit for Mammalian Cells (Thermo Scientific), in accordance with the supplied protocol.

### Citrate Synthase Assay

Mitochondria harvested from each respective condition, as per the Isolation of Mitochondria step, using the Mitochondria Isolation Kit for Mammalian Cells, were then prepared for a citrate synthase assay according to an Oroboros Instruments Laboratory Protocol<sup>82</sup>. Mitochondrial activity was assayed by dispensing 25 $\mu$ L of mitochondria suspension in an incubation medium composed of 775 $\mu$ L deionized H<sub>2</sub>O, 100  $\mu$ L 0.1mM DTNB, 25  $\mu$ L 10% Triton X-100, 50  $\mu$ L oxaloacetate and 25 $\mu$ L acetyl CoA (AcCoA). Absorbance changes representative of the enzymatic activity of citrate synthase was then recorded using a Beckman Coulter DU800 spectrophotometer. Mitochondrial membrane integrity was similarly evaluated using an incubation medium consisting of 800 $\mu$ L H<sub>2</sub>O, 100 $\mu$ L DTNB, 50 $\mu$ L oxaloacetate, 25 $\mu$ L mitochondrial suspension, and 25 $\mu$ L AcCoA.

### Western Blots

Aliquots of total cell lysates containing 60 $\mu$ g protein were dispensed into sodium dodecyl sulfate-polyacrylamide gel and subjected to electrophoresis. After electrophoretic separation, the proteins were then electro-blotted onto nitrocellulose membranes (GE, Hybond –ECL). Blocking was performed with 5% non-fat milk in TBS with 0.1% Tween, or 5% BSA in TBS with 0.1% Tween for phosphoproteins. Membranes were probed with primary antibodies including p-Akt<sup>473</sup>, p-mTOR<sup>Ser792</sup>, and  $\beta$ -actin from Cell Signaling, with p-70S6K from Millipore. Secondary antibodies used included HRP-conjugated mouse and rabbit antibodies (manufacturer and concentrations) and LI-COR IR Dye 680 goat and rabbit antibodies and IR

Dye 800 mouse antibodies, all used at 1:30,000 concentrations. Near-infrared fluorescent western blots were imaged using an Odyssey Imaging System (LI-COR), and rendered into semi-quantitative charts using Image Studio software in conjunction with GraphPad Prism.

## **CHAPTER THREE: RESULTS**

### Reduction of formazan product in proliferation assays in rapamycin-treated conditions

The CellTiter Cell Proliferation Assay used to qualitatively evaluate changes in cell proliferation per growth condition uses a novel tetrazolium compound (MTS) that is presumed to be intracellularly bio-reduced by NADH or NADPH, thus converting the MTS into a formazan product that absorbs at 490nm<sup>83</sup>. Due to the area constraint of the 96-well plate, the preconditioning of cells to new media conditions step was eliminated, opting to simultaneously treat cells with new media conditions plus rapamycin treatment, instead of sequentially. This step appeared vital to generating useable absorbance readings within the tolerances of the reagent and multiplate reader; by restricting the cell population per well, excess formazan production was prevented.

In each of the experimental replicates, the rapamycin-treated conditions exhibited reduced absorbances, attributable to reduced formation of formazan product. In the data supplied by Figure 1, the DMEM, 25mM and 4mM rapamycin conditions had absorbances reduced by 32%  $\pm$ 6.7%, 25% $\pm$ 7.4% and 20% $\pm$ 3.5%, respectively.

These results appeared to be in line with Ramanathan and Schreiber's observation of rapamycin-induced reduction of glycolysis, which would correlate with reduced proliferation. However, cells that rely on aerobic glycolysis as an energy currency/building block generator also have lactate dehydrogenase converting pyruvate and oxidizing NADH to  $\text{NAD}^{+1}$ . A metabolic system primed for oxidizing NADH may provide a case for a false positive interpretation of diminished cellular proliferation. Given conditions of lactic acid fermentation, less NADH is available to reduce MTS to formazan; therefore induced metabolic changes may alter absorbance without necessarily correlating to cellular proliferation differences.

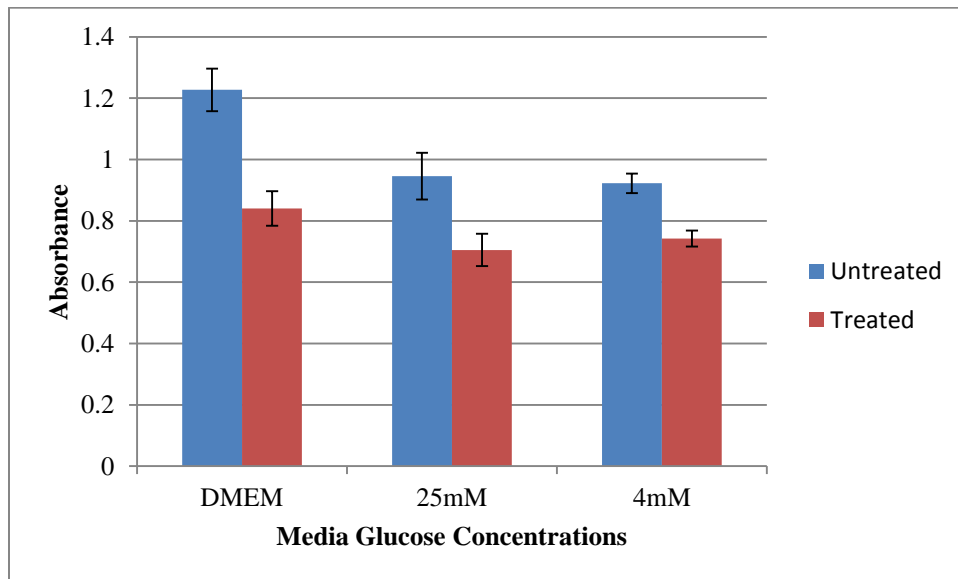


**Figure 1: Absorbance Readings of MTS/Formazan Post Rapamycin Treatment at 490nm**



### Increased ATP concentrations in rapamycin-treated conditions

To examine the effect of nutrient restriction and rapamycin treatment on intracellular energy currency, an assay for quantifying sample ATP concentrations was performed. Following the procedures outlined in Experimental Conditions, six conditions were prepared in a multiwell plate and then assayed according to the ATP Quantification protocol. As per the experimental setup, three media conditions were used: DMEM growth media (25mM glucose, 2mM glutamine), and minimal media at glucose concentrations of 25 and 4mM, respectively, with glutamine concentrations of 0.7mM in each. The growth media condition was used as a contrast in order to compare the ATP concentrations found in each respective media condition, both untreated and treated with 20nM rapamycin.

Decreases in ATP concentrations were found in the untreated minimal media concentrations with reduced glutamine, with respect to the DMEM growth media. Additionally, a decrease in intracellular ATP concentration was observable in the 4mM minimal media versus the 25mM. Notably, each media condition treated with rapamycin was found to have an *increased* ATP concentration versus the untreated conditions. This result appeared to contradict Ramanathan and Schreiber's observation that treatment of cells with rapamycin *decreased* intracellular ATP concentrations immediately after treatment, and for a brief observation period thereafter<sup>69</sup>. Replicate experiments confirmed the repeatability of this phenomenon, thus raising the question of the source of the ATP generation. In the same article, Ramanathan and Schreiber observed that rapamycin-treated cells significantly increased the uptake of amino acids readily converted to TCA intermediates. This information supplied the rationale for the next step: to

evaluate TCA/OXPHOS as a potential candidate for the increase in intracellular ATP in the rapamycin-treated cells.

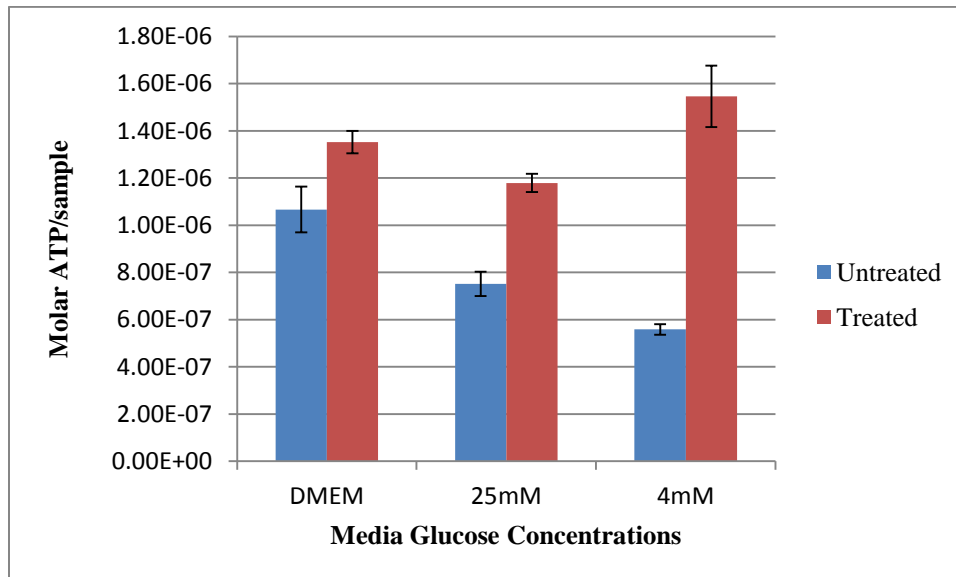


**Figure 2: Molar ATP per Sample, Untreated vs. Treated**

Increased specific activity of citrate synthase in rapamycin-treated conditions

A test for indicating increases in mitochondrially-mediated increases in intracellular ATP via TCA/OXPHOS was derived from an Oroboros Course on High-Resolution Respirometry<sup>82</sup>. This assay required the isolation of mitochondria from cells that were processed according to the Experimental Conditions outlined above, followed by the Isolation of Mitochondria protocol. Thereafter, the isolated mitochondria were assayed using spectrophotometry to observe the activity of citrate synthase, in both lysed and unlysed mitochondrial states. Citrate synthase enacts the first enzymatic step of the TCA, via a conversion of oxaloacetate and acetyl CoA into

citrate and CoASH: Oxaloacetate + Acetyl CoA  $\rightarrow$  Citrate + CoASH. This assay coupled the citrate synthase generation of citrate and CoASH with the reaction of CoASH and a reactive substrate DTNB, as follows: CoASH + DTNB  $\rightarrow$  DTNB-CoA. Specific activity could then be quantified by monitoring the formation of DTNB-CoA, absorbs at 412nm<sup>82</sup>.

The formula for calculating specific activity,  $v$ :  $v = \frac{r_a}{l \cdot \epsilon_B \cdot \nu_B} * \frac{V_{cuvette}}{V_{sample} \cdot \rho}$ , where  $r_a = dA/dt$ , the rate of absorbance change  $\text{min}^{-1}$ ;  $l$ , optical path length = 1 cm;  $\epsilon_B$ , extinction coefficient of B (DTNB) at 412 nm and pH 8.1 =  $13.6 \text{mM}^{-1} \cdot \text{cm}^{-1}$ ;  $\nu_B$ , stoichiometric number of B (TNB) in the reaction = 1;  $V_{cuvette}$ , volume of solution in the cuvette = 1000  $\mu\text{l}$ ;  $V_{sample}$ , volume of sample added to cuvette (100  $\mu\text{l}$ , 25  $\mu\text{l}$ , 5  $\mu\text{l}$ );  $\rho$ , mass concentration or density of biological material in the sample, either protein concentration:  $\text{mg} \cdot \text{cm}^{-3}$  or cell density:  $10^6 \cdot \text{cm}^{-3}$ <sup>82</sup>. Both protein concentration and cell density were used as factors for  $\rho$  in calculating specific activity; with both factors resulting in similar proportions with small variations in total IU per  $10^6$  cells or protein concentrations, respectively. Results were reported in cell density format, as cell count was deemed more reliable an index for  $\rho$ . Bradford assays using total cell lysates from the Isolation of Mitochondria procedure yielded significant variations in protein concentration across replicates, likely attributable to inhomogeneous lysis of cell samples occurring in this step.

Similar to the ATP Quantification experiments, six conditions were tested. However, the DMEM untreated and treated conditions exhibited considerable variability in the quantified citrate synthase specific activity. This variability has been hypothesized to be attributable to the presence of factors present in DMEM but missing in the prepared minimal media. Thus, the

DMEM results have been excluded as a contrast for the 25mM and 4mM minimal media conditions. Despite the variability introduced through artifact in the DMEM conditions, *increased* specific activity of citrate synthase was observed in both rapamycin-treated minimal media conditions in contrast to the untreated conditions.

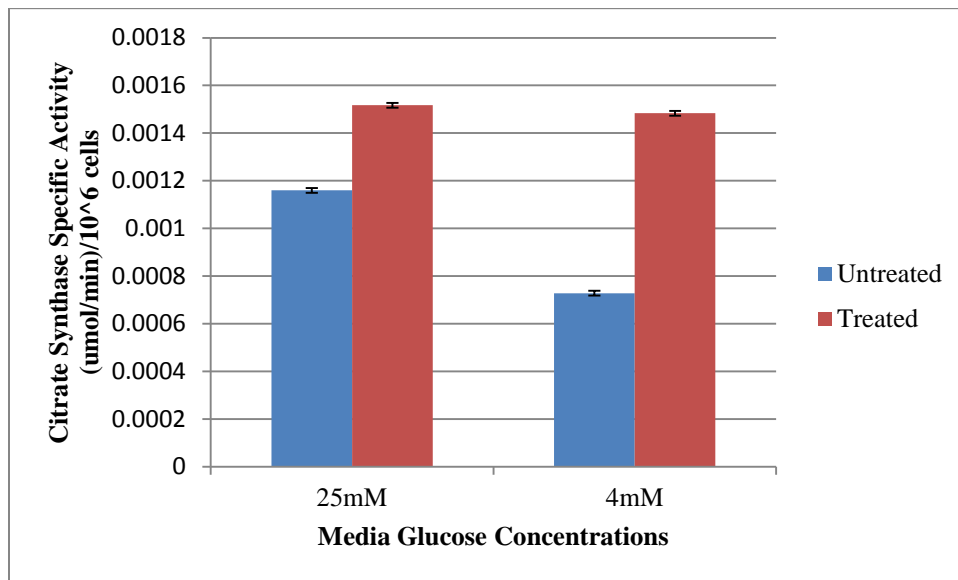


**Figure 3: Mitochondrial Activity Assay, Citrate Synthase Specific Activity in International Units/10<sup>6</sup> cells**

The above experiment assayed for total citrate synthase activity; combined with this assay was an additional spectrophotometric test for mitochondrial membrane integrity. This assay required placement of the isolated mitochondria into a reagent matrix of very similar composition to the activity assay, but eliminated the Triton X-100. By removing detergent from the matrix, the relative integrity of the mitochondrial membranes could be evaluated by the

increases in absorbance due to the permeability/leakiness of the membranes. These experiments indicated that the rapamycin-treated mitochondrial membranes may exhibit slightly *lower* permeability/leakiness than the untreated conditions; however, due to bounds of measurement error and the minuteness of the measurements, these results remain of indeterminate value.

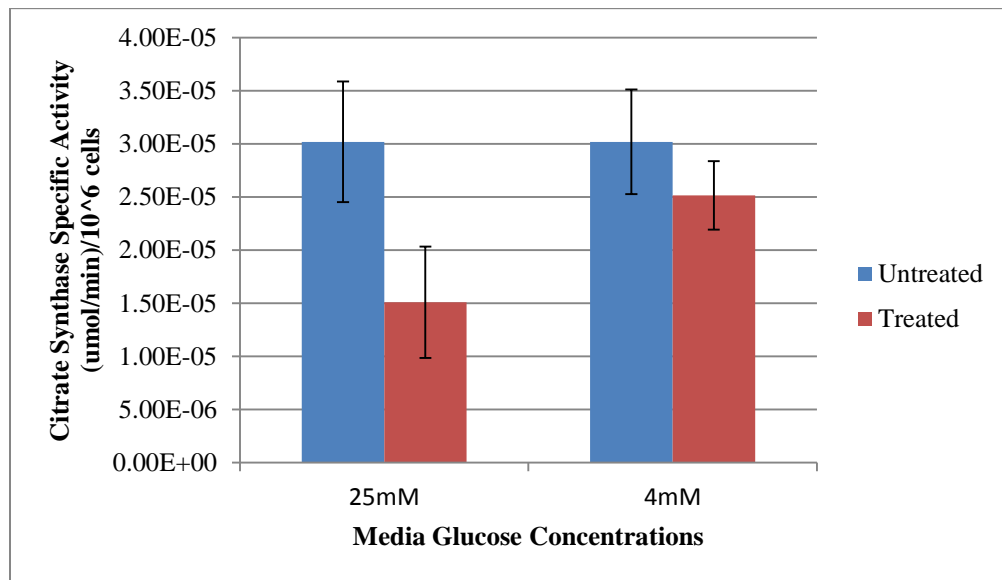


**Figure 4: Mitochondrial Integrity Assay, Citrate Synthase Specific Activity in International Units/10<sup>6</sup> cells**

### Western immunoblots

A series of Western Immunoblots were generated from lysates prepared from cells cultured according to the Experimental Conditions procedure and probed with primary antibodies that would provide insight into the changes of expression and phosphorylation of various metabolic and proliferative proteins. The first of the proteins probed was phospho-

p70S6k, a downstream effector of mTORC1, in order to determine if rapamycin-mediated inhibition of mTORC1 reduced phosphorylation and activation of this key translational protein.

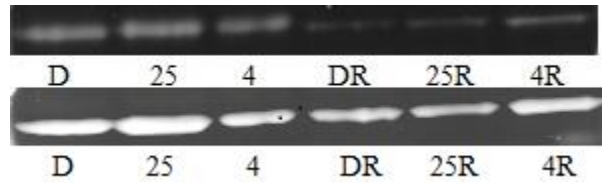


**Figure 5: phospho-70S6 kinase Western immunoblot, β-actin control.** p70S6k above, β-actin below. D = DMEM, 25 = 25mM, 4 = 4mM, DR = DMEM plus rapamycin, 25R = 25mM plus rapamycin, 4R = 4mM plus rapamycin.

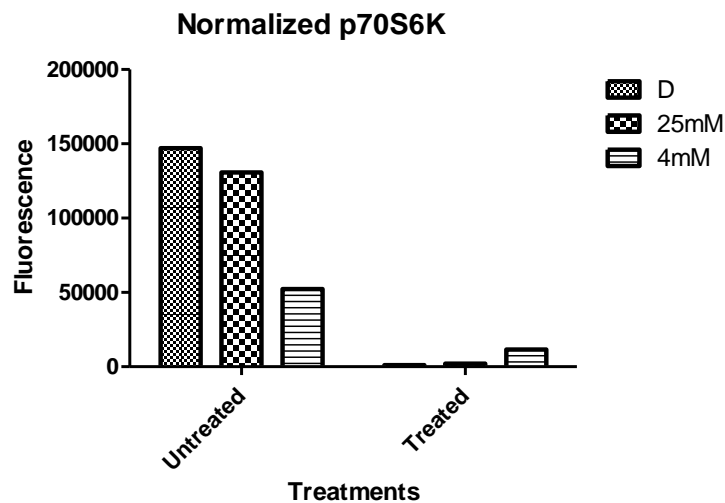


**Figure 6: Semi-quantitative densitometry of phospho-S6 kinase.** From left to right in Untreated category: DMEM, 25mM, 4mM media glucose conditions; in Rapamycin category, DMEM, 2mM, 4mM all treated with 20nM rapamycin.

After normalizing the luminescence values of p70S6K to the  $\beta$ -actin luminescence readings, a number of differences were noted intra-category and between the untreated and treated categories. Firstly, a slight reduction S6K phosphorylation was noted in the untreated category between the growth media DMEM and the 25mM minimal media. A striking difference, however, was noted between the phosphorylation levels of S6K in the 4mM versus the higher glucose concentration media. The 4mM minimal media, untreated, showed nearly a third of the phosphorylation level of S6K compared to the DMEM and 25mM minimal medias. In the rapamycin-treated category, both high glucose media exhibited very weak phosphorylation signals, indicating the inhibitory effect of rapamycin treatment on the phosphorylation of S6K. Notably, the 4mM minimal media treated with rapamycin also showed reduction of phosphorylation compared to untreated conditions, but retained more ~5-10x more phosphorylation of S6K versus the 25mM and DMEM treated conditions, respectively.

The next primary probed was phospho-Akt (Ser 473). In the untreated category, the growth media condition showed much less phosphorylation relative to the 25mM and 4mM media conditions. In the treated category, an *increase* of phosphorylation was noted in the growth media condition, with *decreases* of phosphorylation observed in both 25mM and 4mM compared to the untreated conditions.

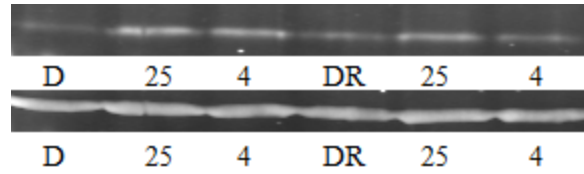


**Figure 7: phospho-Akt (Ser 473),  $\beta$ -actin control.** Phospho-Akt above,  $\beta$ -actin below. D = DMEM, 25 = 25mM, 4 = 4mM, DR = DMEM plus rapamycin, 25R = 25mM plus rapamycin, 4R = 4mM plus rapamycin.

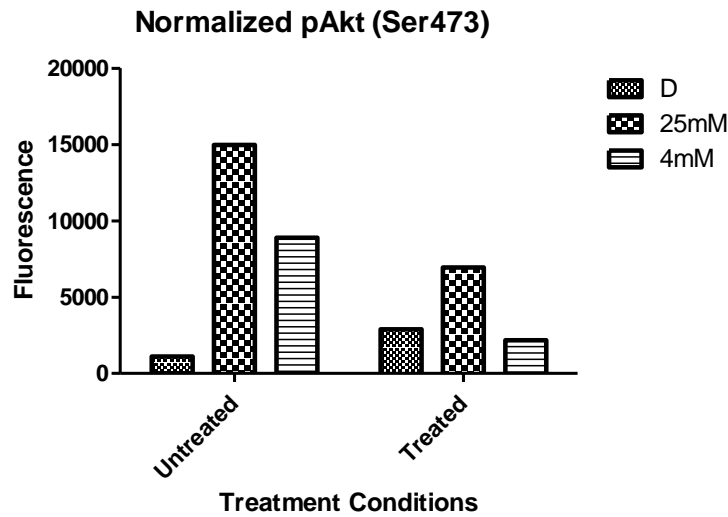


**Figure 8: Semi-quantitative densitometry of phospho-Akt (Ser473).** From left to right in Untreated category: DMEM, 25mM, 4mM media glucose conditions; in Rapamycin category, DMEM, 2mM, 4mM all treated with 20nM rapamycin.

Another vantage on the activity of cell line response to nutrient restriction/rapamycin treatment was provided by the mTORC1-associated protein, Raptor. Raptor is phosphorylated by AMPK on serine residues 722 and 792, which induces inhibition of mTORC1 activity; this phosphorylation occurs in response to AMPK sensing high AMP concentrations relative to ATP<sup>84</sup>. In the untreated conditions, there appeared to be more regulation/inhibition of mTORC1



activity via inhibition of Raptor (Ser792) in the DMEM condition, with less phosphorylation of the residue in both 25mM and 4mM conditions. Paradoxically, in the treated conditions, the 4mM glucose media showed the highest phosphorylation of Raptor, with the DMEM showing negligible and the 25mM condition severely reduced phosphorylations, respectively.

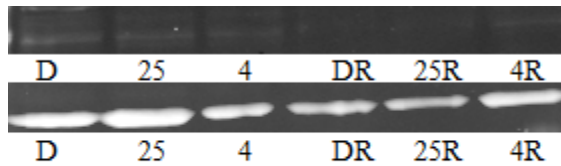


**Figure 9: phospho-Raptor (Ser 792),  $\beta$ -actin control.** Phospho-Raptor above,  $\beta$ -actin below. D = DMEM, 25 = 25mM, 4 = 4mM, DR = DMEM plus rapamycin, 25R = 25mM plus rapamycin, 4R = 4mM plus rapamycin.

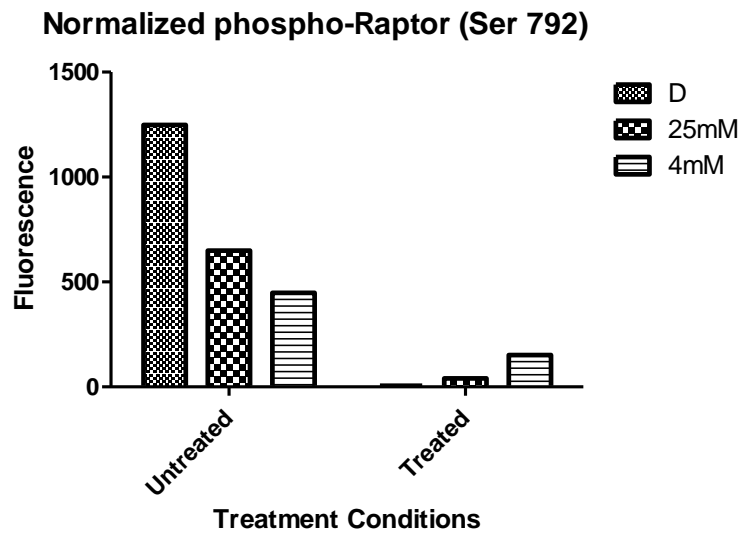


**Figure 10: Semi-quantitative densitometry of phospho-Raptor (Ser792).** From left to right in Untreated category: DMEM, 25mM, 4mM media glucose conditions; in Rapamycin category, DMEM, 2mM, 4mM all treated with 20nM rapamycin.

## CHAPTER FOUR: DISCUSSION

The transgenic P177 myristoylated Akt1 cell line sourced from a murine pancreatic lesion provided a model to evaluate the *in vitro* effects of sequential nutrient restriction and inhibition of mTORC1 on proliferation, expression and metabolism. This cell line offered an opportunity to investigate and potentially manipulate altered cell metabolism in a hyperactivated Akt context, a simulated condition that has been reported in many cancer types. Akt is particularly important in the deregulation of metabolism, factoring importantly in aerobic glycolysis; upon activation, Akt translocates to mitochondria and may contribute to the stimulation of aerobic glycolysis via activation of downstream effectors, such as the phosphorylation of HK II<sup>85,86</sup>. Additionally, Akt figures importantly in the activation of mTOR, which has also been reported to directly control mitochondrial respiration<sup>69</sup>.

An inhibitor of the Akt/mTOR pathway, rapamycin, was used to evaluate the differences in metabolic activity across a set of nutritional conditions. Similarities were observed in the rapamycin-treated conditions with respect to the untreated 4mM glucose minimal media. In particular, reduced phosphorylation of S6K was observed, a key translational protein whose down-regulation would adversely affect proliferation. All rapamycin-treated conditions showed significant de-phosphorylations of p70S6K, with varying responses associated with the nutritional richness of the corresponding media. In particular, rapamycin treatment was associated with reduced phosphorylation of S6K in the higher glucose concentration media compared to the 4mM, reduced glutamine media formula.

The 4mM glucose media formula demonstrated an additional difference when treated with rapamycin, with respect to the phosphorylation status of Raptor (Ser792). Where the DMEM and 25mM treated conditions showed very low to negligible phosphorylation of this residue, the 4mM condition did show phosphorylation, though reduced in contrast to the untreated condition. Most importantly, all treated conditions demonstrate a reduced phosphorylation of Raptor (Ser792), which indicates a reduction of Raptor inhibition. In conditions where mTORC1 is inhibited, the reduced inhibition of Raptor by AMPK in higher glucose concentrations may indicate that a compensatory mechanism bypasses the allosteric effects of rapamycin on mTORC1 function. The phosphorylation of Raptor (Ser792) in the 4mM condition, conversely, appears paradoxical, in that the low glucose conditions would ostensibly be more conducive to a starvation state where the cell has an increased supply of AMP relative to ATP.

Expression differences in phospho-Akt were also noted; probing for this activated protein revealed an apparently additive effect of reduced nutrient supply in combination with rapamycin treatment. Comparing the semi-quantitative data obtained from the Western immunoblots showed that the untreated 4mM media had lower phospho-Akt compared to the 25mM media. Furthermore, both prepared media exhibited reduced phospho-Akt, compared to untreated conditions, when treated with rapamycin. DMEM growth media showed reduced phospho-Akt in contrast to both 25mM and 4mM prepared media conditions, though phospho-Akt increased with rapamycin treatment, relative to the untreated growth media condition. This phenomenon may be explained by the upregulation of Akt as an adaptive response to foreign conditions. The

change from the nutritional excess of the growth media DMEM formulation to the minimal media preparations would require some physiological adjustment on the part of the cell; this response may also account for the increase of phospho-Akt in the growth media conditions due to stress induced by rapamycin treatment. For this reason, cells were preconditioned to new media conditions for a period of 24 hours. This interval provided time for adaptation and allowed the adaptive response to attenuate as the cells equilibrated with the new environment. Additionally, Akt may still be phosphorylated on the Ser473 residue by mTORC2, which is insensitive to rapamycin, or another phosphoinositide dependent kinase 2, such as integrin-linked kinase or p21-activated kinase<sup>92</sup>.

The results of the ATPlite experiments revealed consistent differences in ATP concentrations in untreated versus treated cells across nutritional conditions. The increased concentrations of ATP found in the rapamycin-treated conditions contradicted Ramanathan and Schreiber's finding that rapamycin treatment significantly lowered intracellular ATP concentrations immediately and for up to 25 minutes post-treatment. The hypothesis of this study was based on an expectation that the treated cells would respond similarly to rapamycin and decrease production of ATP. A combination treatment of reduced glucose followed by a reduction of ATP production seemed like a favorable situation to induce an energetic crisis in cells reliant on aerobic glycolysis. In *Direct control of mitochondrial function by mTOR*, the authors state: "Inhibiting mTOR...enhances aerobic glycolysis, but also induces a state of increased dependence on aerobic glycolysis in leukemic cells." The contradictory results of

*increased* ATP concentrations raises additional questions regarding the expectation underlying the hypothesis, as well as the results of Ramanathan and Schreiber's study<sup>69</sup>.

The increased concentrations of ATP after 24 hours of treatment suggested that some alteration in the metabolic system of the cells resulted from rapamycin treatment. A variety of metabolic mechanisms could be responsible for these results; the next step was to identify the potential source of the increased ATP. As TCA/OXPHOS is a much more efficient generator of ATP compared to glycolysis, this pathway seemed like a promising candidate to investigate metabolic changes. Also, Ramanathan and Schreiber noted that cells treated with rapamycin began to increase uptake of amino acids that are readily converted to TCA intermediates<sup>69</sup>. In order to probe the possibility of increases in the TCA/OXPHOS pathway, the citrate synthase specific activity procedure was applied to all conditions.

Consistent results reporting *increased* specific activity of citrate synthase in rapamycin-treated minimal media conditions suggest an increase TCA/OXPHOS pathway activity. However, a response deriving from the TCA/OXPHOS pathway does not indicate an induced metabolic switch from aerobic glycolysis to aerobic respiration. This condition may result as an indirect effect of rapamycin treatment, with alternate energetic pathways compensating for an energy currency deficit. A down-regulation of aerobic glycolytic activity, for example, would generate a different proportion of glycolytic intermediates which could then be consumed by TCA/OXPHOS.

For the purposes of this study, targets immediately upstream and downstream of mTORC1 were selected for analysis. An exhaustive analysis of the signaling pathways could not be accomplished here; however, there are compelling candidates that have been implicated in the signaling/metabolic pathways. For example, inhibition of mTOR has been reported to down-regulate the expression of glycolytic isoenzyme PKM2<sup>81,88</sup>. Reduced expression of PKM2 may consequentially result in increased expression of PKM1, which has a faster reaction rate in generating pyruvate, thus reducing glycolytic intermediate supply for conversion into building blocks. Also, increased production of pyruvate by the higher reaction rate PKM1 would increase available substrate for TCA/OXPHOS.

mTORC1 inhibition has also been shown to induce up-regulation of a microRNA in human cell lines, miR-143; upregulation of miR-143 has been shown to accompany down-regulation of HK II in a variety of mouse and human cancer cell lines<sup>89,90</sup>. A recent study using a human pancreatic cell line (Panc-1) induced an increase in miR-143 and a corresponding decrease in HK II by inhibiting mTORC1 with a rapamycin analog, everolimus. Additionally, Panc-1 cells treated with everolimus demonstrated lower levels of lactate dehydrogenase activity and lactate production versus untreated cells. The authors conclude that inhibition of mTORC1 signaling results in an *inhibition* of glycolysis<sup>91</sup>. Such a conclusion, however, oversimplifies the complexity of the cellular expression response to mTORC1 inhibition. Reduced turnover rate of pyruvate may result from higher  $K_m$  hexokinase isoenzymes that are expressed in compensation to the miR-143 inhibited HK II. Such a result does not necessarily correspond to inhibition of glycolysis, instead potentially reflecting an expression-induced change of rate.

The fact that *increased* ATP is observed in contradistinction to Ramanathan and Schreiber's observation of *decreased* ATP as an immediate response to rapamycin exposure may indicate that the above authors captured a *transitional* step in metabolic switching in response to mTOR inhibition. The discovery of miR-143-mediated down-regulation of glycolysis offers support for this possibility. In particular, the decrease of lactate dehydrogenase (LDH) activity in the everolimus-treated Panc-1 cells suggests a reversion of the glycolytic pathway from aerobic to typical glycolysis. With less LDH activity converting pyruvate to lactic acid, a greater supply of pyruvate would remain available as substrate for mitochondrial conversion via TCA/OXPHOS.

The results of the experiments listed for this study do not readily conform to the expectations of the proposed hypothesis: a combination treatment of nutrient restriction and rapamycin inhibition will exert an additive or synergistic cytostatic/cytotoxic effect *in vitro* on the mAkt1 pancreatic early lesion cell line. What seems probable, given the results and with new information about the effects of miR-143, is a situation of reduced cellular proliferation in cells exhibiting aerobic glycolysis when treated with rapamycin. Restriction of nutrients in combination with inhibition of mTOR signaling seems likely to further reduce proliferation due to reduced supply of building blocks. This reformulated proposal can be tested using carboxyfluorescein succinimidyl ester (CFSE) dye in conjunction with flow cytometry. Another proposal is to identify the mechanisms responsible for metabolic conversion, discerning if a conversion from aerobic glycolysis to typical glycolysis occurs in response to mTOR inhibition. This could be tested by quantifying glycolysis reaction rate and identifying isoenzyme

expression with respect to treatment conditions. Lastly, changes can be tracked in TCA/OXPHOS activity as a response to mTOR inhibition and varying nutrient conditions.

## CHAPTER FIVE: CONCLUSION

In summary, nutrient restriction *in vitro* appears to exert some similar effects to rapamycin-mediated inhibition of mTORC1. Nutrient availability, glucose and glutamine in particular, impacts phosphorylation states of S6K, and consequently processes of translation. The increases in ATP concentration may potentially be attributable to an increase in TCA/OXPHOS; the increased citrate synthase activity provides a suggestive clue to this possibility. However, the increased specific activity of this enzyme does not conclusively demonstrate the switching of metabolic emphasis from glycolysis to TCA/OXPHOS. Thus, a necessary future direction is to directly monitor the extracellular acidification rate (ECAR) and oxygen consumption rate (OCR) of the six defined conditions to determine if a metabolic switching occurs in the process of rapamycin treatment, and if nutrient restriction additively or negatively contributes to such a conversion.

### Future Directions

The measurement of ECAR and OCR per condition will be necessary to determine if the increased source of intracellular ATP can be attributed to increased mitochondrial function. This step will be performed with a Seahorse Biosciences XF<sup>e</sup>24 extracellular flux machine, and tested with a glycolysis stress kit.



Confirmatory results of reduced proliferation with respect to nutrient conditions intracategorically, and also versus rapamycin-treated conditions can be more accurately assessed using carboxyfluorescein succinimidyl ester (CFSE), a fluorescent dye used in flow cytometry to quantify cell proliferation. Upon cellular uptake and modification of this dye, CFSE cannot readily leave the cell. As a result, upon cellular division, the dye is distributed between daughter cells. Peak fluorescent intensity supplies information on the degree of proliferation that has occurred; high intensity peak indicates low proliferation, lower intensity, with a broader distribution or peak area indicates increased proliferation. This test would provide significantly improved quantitation of reduced proliferation in either nutrient-restricted or rapamycin-treated conditions.

Western blots will also be generated showing total AKT, total S6K and total Raptor in order to relate expression levels to phosphorylation levels.

## LIST OF REFERENCES

1. Voet DJ, Voet, JG, Pratt, CW. Fundamentals of Biochemistry. 3<sup>rd</sup> Ed. John Wiley & Sons, Inc.; 2008. p. 448-529.
2. Ko YH, Delannoy M, Hullihen J, Chiu W, Pedersen PL. Mitochondrial ATP synthasome. Cristae-enriched membranes and a multiwell detergent screening assay yield dispersed single complexes containing the ATP synthase and carriers for Pi and ADP/ATP. *J Biol Chem.* 2003;278(14):12305-9.
3. Voet DJ, Voet, JG, Pratt, CW. Fundamentals of Biochemistry. 3<sup>rd</sup> Ed. John Wiley & Sons, Inc.; 2008. p. 566-639.
4. Smolková K, Plecítá-Hlavatá L, Bellance N, Benard G, Rossignol R, Ježek P. Waves of gene regulation suppress and then restore oxidative phosphorylation in cancer cells. *Int J Biochem Cell Biol.* 2011;43(7):950-68.
5. Warburg, O, Posener, K, Negelein, E. Über den Stoffwechsel der Carcinomzelle. *Biochem Zeitschr.* 1924;52:309–344. Translated from German.
6. Koppenol, WH, Bounds, PL, Dang, CV. Otto Warburg's contributions to current concepts of cancer metabolism. *Nat Rev Cancer.* 2011;11:325-337.
7. Warburg, O. Über den heutigen Stand des Carcinomproblems. *Naturwiss.* 1927;15:1-4. Translated from German.
8. Petros JA, Baumann AK, Ruiz-Pesini E, Amin MB, Sun CQ, Hall J, Lim S, Issa MM, Flanders WD, Hosseini SH, Marshall FF, Wallace DC. mtDNA mutations increase tumorigenicity in prostate cancer. *Proc Natl Acad Sci USA.* 2005;102(3):719-24.
9. Zhou S, Kachhap S, Sun W, Wu G, Chuang A, Poeta L, Grumbine L, Mithani SK, Chatterjee A, Koch W, Westra WH, Maitra A, Glazer C, Carducci M, Sidransky D, McFate T, Verma A, Califano JA. Frequency and phenotypic implications of mitochondrial DNA mutations in human squamous cell cancers of the head and neck. *Proc Natl Acad Sci U S A.* 2007;104(18):7540-5.
10. Altenberg B., Greulich KO. Genes of glycolysis are ubiquitously overexpressed in 24 cancer classes. *Genomics.* 2004;84, 1014–1020.
11. Demetrius LA, Coy JF, Tuszynski JA. Cancer proliferation and therapy: the Warburg effect and quantum metabolism. *Theor Biol Med Model.* 2010;7:2.

12. Warburg O. On respiratory impairment in cancer cells. *Science*. 1956;124(3215):269-70.
13. Pedersen PL. Warburg, me and Hexokinase 2: Multiple discoveries of key molecular events underlying one of cancers' most common phenotypes, the "Warburg Effect", i.e., elevated glycolysis in the presence of oxygen. *J Bioenerg Biomembr*. 2007;39:211–222
14. Mathupala SP, Ko YH, Pedersen, PL. Hexokinase II: Cancer's double-edged sword acting as both facilitator and gatekeeper of malignancy when bound to mitochondria. *Oncogene*. 2006;25:4777–4786
15. Dang CV. Role of aerobic glycolysis in genetically engineered mouse models of cancer. *BMC Biology*. 2013;11:3
16. Rempel A, Bannasch P, Mayer D. Differences in expression and intracellular distribution of hexokinase isoenzymes in rat liver cells of different transformation stages. *Biochim Biophys Acta*. 1994;1219:660–668.
17. Pedersen PL., Mathupala S, Rempel A, Geschwind JF, Ko YH. Mitochondrial bound type II hexokinase: a key player in the growth and survival of many cancers and an ideal prospect for therapeutic intervention. *Biochim Biophys Acta*. 2002;1555:14–20.
18. Postic C, Shiota M, Magnuson MA. Cell-specific roles of glucokinase in glucose metabolism. *Recent Prog Horm Res*. 2001;56:195-217.
19. Iynedjian, PB. Molecular Physiology of Mammalian Glucokinase. *Cell Mol Life Sci*. 2009 Jan;66(1):27–42.
20. Stubbs M, Aiston S, Agius L. Subcellular Localization, Mobility, and Kinetic Activity of Glucokinase in Glucose-Responsive Insulin-Secreting Cells. *Diabetes*. 2000;49:2048-2055
21. Danial NN, Gramm CF, Scorrano L, Zhang CY, Krauss S, Ranger AM, Datta SR, Greenberg ME, Licklider LJ, Lowell BB, Gygi SP, Korsmeyer SJ. BAD and glucokinase reside in a mitochondrial complex that integrates glycolysis and apoptosis. *Nature*. 2003;424:952–956.
22. Wilson, JE. Isozymes of mammalian hexokinase: structure, subcellular localization and metabolic function. *The Journal of Experimental Biology*. 2003;206:2049-2057.
23. Arora KK, Pedersen, PL. Functional significance of mitochondrial bound hexokinase in tumor cell metabolism. Evidence for preferential phosphorylation of glucose by intramitochondrially generated ATP. *J Biol Chem*. 1988;263:17422-17428.

24. BeltrandelRio H, Wilson JE. Hexokinase of rat brain mitochondria: relative importance of adenylate kinase and oxidative phosphorylation as sources of substrate ATP, and interaction with intramitochondrial compartments of ATP and ADP. *Arch Biochem Biophys.* 1991;286(1):183-94.
25. Azoulay-Zohar H, Israelson A, Abu-Hamad S, Shoshan-Barmatz V. In self-defence: hexokinase promotes voltage-dependent anion channel closure and prevents mitochondria-mediated apoptotic cell death. *Biochem J.* 2004;377(Pt 2):347-55.
26. de Cerqueira Cesar M, Wilson JE. Functional characteristics of hexokinase bound to the type a and type B sites of bovine brain mitochondria. *Arch Biochem Biophys.* 2002;397(1):106-12.
27. Mazurek S. Pyruvate kinase type M2: A key regulator of the metabolic budget system in tumor cells. *Int J Biochem. Cell Biol.* 2011;43:969–980.
28. Yamada K, Noguchi T. Regulation of pyruvate kinase M gene expression. *Biochem Biophys Res Commun.* 1999;256(2):257-62.
29. Vander Heiden, MG, Cantley, LC, Thompson, CB. Understanding the Warburg Effect: The Metabolic Requirements of Cell Proliferation. *Science.* 2009;324(5930): 1029–1033.
30. Ward PS, Thompson CB. Metabolic Reprogramming: A Cancer Hallmark Even Warburg Did Not Anticipate. *Cancer Cell.* 2012;21: 297-308.
31. Spodena GA, Rosteka U, Lechnera S, Mitterbergera, M, Mazurekc, S, Zwerschkea, W. Pyruvate kinase isoenzyme M2 is a glycolytic sensor differentially regulating cell proliferation, cell size and apoptotic cell death dependent on glucose supply. *Exp Cell Res.* 2009;315: 2765-2774.
32. Anastasiou D, Poulogiannis G, Asara JM, Boxer MB, Jiang JK, Shen M, Bellinger G, Sasaki AT, Locasale JW, Auld DS, Thomas CJ, Vander Heiden MG, Cantley LC. Inhibition of pyruvate kinase M2 by reactive oxygen species contributes to cellular antioxidant responses. *Science.* 2011;334(6060):1278-83.
33. Hitosugi T, Kang S, Vander Heiden MG, et al. Tyrosine Phosphorylation Inhibits PKM2 to Promote the Warburg Effect and Tumor Growth. *Sci Signal.* 2009; 2(97): ra73.
34. Lv L, Li D, Zhao D, Lin R, Chu Y, Zhang H, Zha Z, Liu Y, Li Z, Xu Y, Wang G, Huang Y, Xiong Y, Guan KL, Lei QY. Acetylation targets the M2 isoform of pyruvate kinase for degradation through chaperone-mediated autophagy and promotes tumor growth. *Mol Cell.* 2011;42(6):719-30.

35. Altomare DA, Testa JR. Perturbations of the AKT signaling pathway in human cancer. *Oncogene*. 2005;24:7455–64.
36. Cicens J. The potential role of Akt phosphorylation in human cancers. *Int J Biol Markers*. 2008;23:1-9.
37. Gonzalez E, McGraw TE. The Akt kinases: isoform specificity in metabolism and cancer. *Cell Cycle*. 2009;8(16):2502-8.
38. Heron-Milhavet, L, Khouya, N, Fernandez, A, Lamb, NJ. Akt1 and Akt2: Differentiating the aktion. *Histol Histopathol*. 2011;26: 651-662.
39. Pastorino, JG, Hoek, JB. Regulation of hexokinase binding to VDAC. *J Bioenerg Biomembr*. 2008;40:171–182
40. Elstrom RL, Bauer DE, Buzzai M, Karnauskas R, Harris MH, Plas DR, Zhuang H, Cinalli RM, Alavi A, Rudin CM et al. Akt stimulates aerobic glycolysis in cancer cells. *Cancer Res*. 2004;64:3892–3899
41. Miyamoto S, Murphy AN, Brown JH. Akt mediates mitochondrial protection in cardiomyocytes through hosphorylation of mitochondrial hexokinase-II. *Cell Death Differ*. 2008;15:521–529
42. Kohn AD, Takeuchi F, Roth RA. Akt, a pleckstrin homology domain containing kinase, is activated primarily by phosphorylation. *J Biol Chem*. 1996;271(36):21920-6.
43. Kohn AD, Summers SA, Birnbaum MJ, Roth RA. Expression of a Constitutively Active Akt Ser/Thr Kinase in 3T3-L1 Adipocytes Stimulates Glucose Uptake and Glucose Transporter 4 Translocation. *J Biol Chem*. 1996;271(49):31372-8.
44. Manning BD, Cantley LC. AKT/PKB Signaling: Navigating Downstream. *Cell*. 2007 Jun 29;129(7):1261-74.
45. Altomare DA, Khaled AR. Homeostasis and the Importance for a Balance Between AKT/mTOR Activity and Intracellular Signaling. *Curr Med Chem*. 2012;19(22):3748-62.
46. Manning BD, Cantley LC. Rheb fills a GAP between TSC and TOR. *Trends Biochem Sci* 2003;28:573–576.
47. Sancak Y, Thoreen CC, Peterson TR, Lindquist RA, Kang SA, Spooner E, Carr SA, Sabatini DM. PRAS40 is an insulin-regulated inhibitor of the mTORC1 protein kinase. *Mol Cell* 2007;25:903–915.

48. Zhou HY, Huang SL. Current development of the second generation of mTOR inhibitors as anticancer agents. *Chin J Cancer*. 2012;31(1):8-18.
49. O'Reilly KE, Rojo F, She QB, Solit D, Mills GB, Smith D, Lane H, Hofmann F, Hicklin DJ, Ludwig DL, Baselga J, Rosen N. mTOR inhibition induces upstream receptor tyrosine kinase signaling and activates Akt. *Cancer Res*. 2006;66(3):1500-8.
50. Um SH, Frigerio F, Watanabe M, Picard F, Joaquin M, Sticker M, Fumagalli S, Allegrini PR, Kozma SC, Auwerx J, Thomas G. Absence of S6K1 protects against age- and diet-induced obesity while enhancing insulin sensitivity. *Nature*. 2004;431(7005):200-5.
51. Zick Y. Ser/Thr phosphorylation of IRS proteins: a molecular basis for insulin resistance. *Sci STKE*. 2005;2005(268):pe4.
52. Mathew R, White E. Autophagy in tumorigenesis and energy metabolism: friend by day, foe by night. *Curr Opin Genet Dev*. 2011;21(1):113-9.
53. Jung CH, Ro SH, Cao J, Otto NM, Kim DH. mTOR regulation of autophagy. *FEBS Lett*. 2010;584(7):1287-95.
54. Shaw RJ, Bardeesy N, Manning BD, Lopez L, Kosmatka M, DePinho RA, Cantley LC. The LKB1 tumor suppressor negatively regulates mTOR signaling. *Cancer Cell*. 2004;6(1):91-9.
55. Hardie, DG. Sensing of energy and nutrients by AMP-activated protein kinase1–4. *Am J Clin Nutr* 2011;93:1891S–6S.
56. Ma XM, Blenis J. Molecular mechanisms of mTOR-mediated translational control. *Nat Rev Mol Cell Biol*. 2009;10:307–318.
57. Gingras AC, Kennedy SG, O'Leary MA, Sonenberg N, Hay N. 4E-BP1, a repressor of mRNA translation, is phosphorylated and inactivated by the Akt(PKB) signaling pathway. *Genes Dev*. 1998;12:502–513.
58. Goo CK, Lim HY, Ho QS, Too HP, Clement MV, Wong KP. PTEN/Akt Signaling Controls Mitochondrial Respiratory Capacity through 4E-BP1. *PLoS One*. 2012;7(9):e45806.
59. Meyuhas O. Synthesis of the translational apparatus is regulated at the translational level. *Eur J Biochem*. 2000;267(21):6321-30.
60. Hara K, Yonezawa K, Weng QP, Kozlowski MT, Belham C, Avruch J. Amino acid sufficiency and mTOR regulate p70 S6 kinase and eIF-4E BP1 through a common effector mechanism. *J Biol Chem*. 1998;273(23):14484-94.

61. Yellen P, Chatterjee A, Preda A, Foster DA. Inhibition of S6 kinase suppresses the apoptotic effect of eIF4E ablation by inducing TGF- $\beta$ -dependent G1 cell cycle arrest. *Cancer Lett.* 2013; S0304-3835(13)00087-6.
62. Yellen P, Saqcena M, Salloum D, Feng J, Preda A, Xu L, Rodrik-Outmezguine V, Foster DA. High-dose rapamycin induces apoptosis in human cancer cells by dissociating mTOR complex 1 and suppressing phosphorylation of 4E-BP1. *Cell Cycle.* 2011 Nov 15;10(22):3948-56.
63. Scheffler IE. Mitochondria make a come back. *Adv Drug Deliv Rev.* 2001 Jul 2;49(1-2):3-26.
64. Baltzer C, Tiefenböck SK, Frei C. Mitochondria in response to nutrients and nutrient-sensitive pathways. *Mitochondrion.* 2010;10(6):589-97.
65. Desai BN, Myers BR, Schreiber SL. FKBP12-rapamycin-associated protein associates with mitochondria and senses osmotic stress via mitochondrial dysfunction. *Proc Natl Acad Sci USA.* 2002;99:4319-4324.
66. Schieke SM, Phillips D, McCoy JP, Aponte AM, Shen RF, Balaban RS, Finkel T. The mammalian target of rapamycin (mTOR) pathway regulates mitochondrial oxygen consumption and oxidative capacity. *J Biol Chem.* 2006 Sep 15;281(37):27643-52.
67. Sarbassov DD, Ali SM, Sabatini DM. Growing roles for the mTOR pathway. *Curr Opin Cell Biol.* 2005;17(6):596-603.
68. Wullschleger S, Loewith R, Hall MN. TOR signaling in growth and metabolism. *Cell.* 2006;10;124(3):471-84.
69. Ramanathan A, Schreiber SL. Direct control of mitochondrial function by mTOR. *Proc Natl Acad Sci U S A.* 2009 Dec 29;106(52):22229-32.
70. Hirayama A, Kami K, Sugimoto M, Sugawara M, Toki N, Onozuka H, Kinoshita T, Saito N, Ochiai A, Tomita M, Esumi H, Soga T. Quantitative metabolome profiling of colon and stomach cancer microenvironment by capillary electrophoresis time-of-flight mass spectrometry. *Cancer Res.* 2009 Jun 1;69(11):4918-25.
71. Medina MA. Glutamine and cancer. *J Nutr.* 2001 Sep;131(9 Suppl):2539S-42S.
72. DeBerardinis RJ, Cheng T. Q's next: the diverse functions of glutamine in metabolism, cell biology and cancer. *Oncogene.* 2010;29:313-324.

73. Dang CV. Glutaminolysis: supplying carbon or nitrogen or both for cancer cells? *Cell Cycle*. 2010;9:3884–3886.
74. Dang CV. Rethinking the Warburg effect with Myc micromanaging glutamine metabolism. *Cancer Res*. 2010;70:859–862.
75. Fujii S, Mitsunaga S, Yamazaki M, Hasebe T, Ishii G, Kojima M, et al. Autophagy is activated in pancreatic cancer cells and correlates with poor patient outcome. *Cancer Sci*. 2008;99(9):1813-9.
76. Wu CA, Chao Y, Shiah SG, Lin WW. Nutrient deprivation induces the Warburg effect through ROS/AMPK-dependent activation of pyruvate dehydrogenase kinase. *Biochim Biophys Acta*. 2013;1833(5):1147-1156.
77. Lu J, Kunimoto S, Yamazaki Y, Kaminishi M, Esumi H. Kigamicin D, A novel anticancer agent based on a new anti-austerity strategy targeting cancer cells' tolerance to nutrient starvation. *Cancer Sci*. 2004;95(6):547-52.
78. Aki T, Yamaguchi K, Fujimiya T, Mizukami Y. Phosphoinositide 3-kinase accelerates autophagic cell death during glucose deprivation in the rat cardiomyocyte-derived cell line H9c2. *Oncogene*. 2003;22(52):8529-35.
79. Wu YT, Tan HL, Huang Q, Ong CN, Shen HM. Activation of the PI3K-Akt-mTOR signaling pathway promotes necrotic cell death via suppression of autophagy. *Autophagy*. 2009;5(6):824-34.
80. Lashinger LM, Malone LM, Brown GW, Daniels EA, Goldberg JA, Otto G, Fischer SM, Hursting SD. Rapamycin partially mimics the anticancer effects of calorie restriction in a murine model of pancreatic cancer. *Cancer Prev Res (Phila)*. 2011;4(7):1041-51.
81. Sun Q, Chen X, Ma J, Peng H, Wang F, Zha X, Wang Y, Jing Y, Yang H, Chen R, Chang L, Zhang Y, Goto J, Onda H, Chen T, Wang MR, Lu Y, You H, Kwiatkowski D, Zhang H. Mammalian target of rapamycin up-regulation of pyruvate kinase isoenzyme type M2 is critical for aerobic glycolysis and tumor growth. *Proc Natl Acad Sci USA*. 2011;108(10):4129-34.
82. Kuznetsov, A, Lassnig, B, Gnaiger, E. Course on High-Resolution Respirometry. 2003. Oroboros Instruments; Mitochondrial Physiology Network 8.14.
83. Promega. Technical Bulletin: CellTiter 96® Aqueous One Solution Cell Proliferation Assay: Instructions for use of products G3580, G3581 AND G3582. 2012; 1-2.



84. Gwinn DM, Shackelford DB, Egan DF, Mihaylova MM, Mery A, Vasquez DS, Turk BE, Shaw RJ. AMPK phosphorylation of raptor mediates a metabolic checkpoint. *Mol Cell*. 2008;30(2):214-26.
85. Bijur GN, Jope RS. Rapid accumulation of Akt in mitochondria following phosphatidylinositol 3-kinase activation. *J Neurochem*. 2003;87(6):1427-35.
86. Elstrom RL, Bauer DE, Buzzai M, Karnauskas R, Harris MH, et al. Akt stimulates aerobic glycolysis in cancer cells. *Cancer Res*. 2004;64(11):3892-9.
87. Li C, Liu Y, Liu J, Chen Y, Li Z, Chen X, et al. Rapamycin inhibits human glioma cell proliferation through down-regulating mammalian target of rapamycin pathway and up-regulating microRNA-143. *Head Neck Oncol*. 2012;4(3):66.
88. Iqbal MA, Bamezai RN. Resveratrol inhibits cancer cell metabolism by down regulating pyruvate kinase M2 via inhibition of mammalian target of rapamycin. *PLoS One*. 2012;7(5):e36764.
89. Li C, Liu Y, Liu J, Chen Y, Li Z, Chen X, Yang K, Li M, Liu Z. Rapamycin inhibits human glioma cell proliferation through down-regulating mammalian target of rapamycin pathway and up-regulating microRNA-143. *Head Neck Oncol*. 2012;4(3):66.
90. Fang R, Xiao T, Fang Z, Sun Y, Li F, Gao Y. MicroRNA-143 (miR-143) regulates cancer glycolysis via targeting hexokinase 2 gene. *J Biol Chem*. 2012;287(27):23227-35.
91. Liu L, Gong L, Zhang Y, Li N. Glycolysis in Panc-1 human pancreatic cancer cells is inhibited by everolimus. *Exp Ther Med*. 2013;5(1):338-342.
92. Dong LQ, Liu F. PDK2: the missing piece in the receptor tyrosine kinase signaling pathway puzzle. *Am J Physiol Endocrinol Metab*. 2005;289(2):E187-96.